THE ASTROPHYSICAL JOURNAL, 503:792–797, 1998 August 20
© 1998. The American Astronomical Society. All rights reserved. Printed in U.S.A.

THE STRUCTURE OF COMETARY KNOTS IN THE HELIX NEBULA[1]

A. BURKERT[2] AND C. R. O'DELL[2,3]

Received 1997 November 3; accepted 1998 March 17

ABSTRACT

The Hα surface brightness distribution of cometary knots in the Helix Nebula is investigated. The brightness profiles of their photoionized surfaces (cusps) drop exponentially with increasing distance r from the center of the knots: $\Sigma(r) \sim \exp(-r/h)$. An r^{-3} profile, which would be expected for a freely expanding ionization region, in general does not provide a good fit. The cusps of all the knots have the same universal exponential brightness scale height h of 2 pixels (6.3×10^{14} cm), which is also independent of the direction with respect to the central star. The origin of the cometary knots and the formation and nature of their luminous cusps is investigated. We propose that the cusps are in hydrostatic equilibrium rather than freely expanding, but we have been unable to identify a physical mechanism that will constrain them. Lyα radiation pressure acting on the dust is evaluated as a mechanism to do the confinement, but it lacks sufficient energy density, and the scale height expected disagrees with what is observed.

Subject headings: ISM: structure — planetary nebulae: individual (NGC 7293) — stars: mass loss

1. INTRODUCTION

The Helix Nebula (NGC 7293) is one of the closest planetary nebulae (PN), at a distance of 213 pc (Harris 1997). As one of the largest and oldest objects with a radius of order 0.37 pc and an expansion age of 17,000 yr, it is an ideal candidate for studying the structure of PN in the late stage of their evolution.

Recent imaging with the *HST* Wide Field and Planetary Camera 2 (WFPC2) (O'Dell & Handron 1996, hereafter OH96; O'Dell & Burkert 1997) has resolved in detail the filamentary fine scale structure originally detected by Walter Baade (Vorontzov-Velyaminov 1968), the basic nature of which was determined by Meaburn et al. (1992) and Walsh & Meaburn (1993) from ground-based images. The filaments, called cometary knots (CK), are characterized by a central dark core seen in silhouette against the background nebular emission, by a luminous cusp on the substellar side, and by a thin sheath of luminous material extending from the edge of the cusp to larger distances. That the central dark knots consist of high-density neutral and molecular gas is inferred from their extinction of the background radiation (Meaburn et al. 1992; OH96) and from radio observations of the CO (Huggins et al. 1992) and C I lines (Young et al. 1997). The cusps represent photoionized surfaces that are optically thick to the Lyman continuum radiation. Their peak surface brightness in Hα shows the expected $1/d^2$ decay with increasing distance d from the central star (OH96). The cometary tails, which point radially away from the central star, probably result from ionized gas within the cusps that is stripped by some radial force.

OH96 have argued that the Hα surface brightness of the photoionized cusps drops exponentially with increasing distance r from the knot. This result is puzzling, since simple equilibrium outflow models (Dyson 1968) would predict an r^{-2} density distribution, leading in projection to an r^{-3} surface brightness profile. If confirmed, this result would provide important information about the origin of the cusps, their surroundings, and the stripping mechanism.

In this paper we present a detailed analysis of the projected two-dimensional structure of the CK in the Helix Nebula. Section 2 will summarize the observations, which are analyzed in § 3. A discussion of the results and a model for the origin of the universal cusp profiles is presented in § 4.

2. THE OBSERVATIONAL MATERIAL

The data used in this analysis derive from two *Hubble Space Telescope* (*HST*) WFPC2 programs involving the second author. GTO program 5086 imaged a section in the inner ring of the north portion of the nebula (OH96), and GO program 5311 imaged a contiguous field to the east (O'Dell & Burkert 1997). Observations were made in the narrowband filters, isolating the [O III] line at 5007 Å, the [N II] line at 6583 Å, and the Hα line at 6563 Å. Additional observations were made in the nebular continuum in the intermediate band filters near the V bandpass with the F547M filter, which has a peak transmission near 5470 Å. A color-coded composite image in the emission lines appears with our earlier article (O'Dell & Burkert 1997). At the adopted distance of the Helix Nebula (213 pc), the WFPC2 pixel size of 0.″0996 projects to 3.17×10^{14} cm.

Since our analysis requires flux-calibrated images, we corrected the Hα image for the contribution made by the two nearby [N II] lines at 6548 and 6583 Å and a smaller contribution from the nebular continuum. The details of the method appear in Handron (1995) and O'Dell (1998). This method of calibration relies on WFPC2 prelaunch calibration numbers only secondarily, primarily using observations of the Orion Nebula as the flux standard. The final result was an emission-line image in Hα in units of photons cm^{-2} s^{-1} sr^{-1}. Throughout this analysis we used the IRAF[4] data reduction package. Eight particular CK were selected for detailed analysis. They were chosen primarily on the basis of being isolated from similar objects or fea-

[1] Based on observations made with the NASA/ESA *Hubble Space Telescope*, obtained at the Space Telescope Science Institute, which is operated by the Association of Universities for Research in Astronomy, Inc., under NASA contract NAS 5-26555.

[2] Max-Planck-Institut für Astronomie, Königstuhl 17, D-69117 Heidelberg, Germany; burkert@mpia-hd.mpg.de.

[3] Department of Space Physics and Astronomy, MS-108 Rice University, 6100 South Main Street, Houston, TX 77005-1892; cro@rice.edu.

[4] IRAF is distributed by the National Optical Astronomy Observatories, which is operated by the Association of Universities for Research in Astronomy, Inc., under cooperative agreement with the National Science foundation.

TABLE 1

PHYSICAL PROPERTIES OF THE KNOTS

Knot	d	R_k	h	$\log \Sigma_{max}$
352-815.....	126.8	6.75	1.95 ± 0.25	7.94
358-800.....	138.3	7.5	1.8 ± 0.20	7.75
360-751.....	147.2	9.5	1.7 ± 0.30	7.73
378-801.....	132.4	6.2	2.3 ± 0.10	7.87
386-749.....	144.0	5.5	1.6 ± 0.40	7.76
398-752.....	142.2	6.5	2.5 ± 0.60	7.76
428-900.....	94.7	10	2.0 ± 0.20	7.84
473-931.....	130.4	9.0	1.8 ± 0.25	7.76

NOTE.—Sample of cometary knots with some characteristic properties: d, distance to central star in pixels; R_k, knot radius in pixels; h, exponential cusp scale height in pixels; Σ_{max}, maximum cusp Hα surface brightness in photons cm^{-2} s^{-1} sr^{-1}.

tures associated with the main body of the nebula, thus allowing the best opportunity to determine the background that must be subtracted. The knots and some of their physical properties are summarized in Table 1. Here we adopt the system of designation proposed by O'Dell & Burkert (1997), identifying a knot by its right ascension in units of $0^s.1$ (first three digits) and by its declination in units of $1''$ (last three digits).

3. DATA ANALYSIS

The two-dimensional surface brightness structure of the CK is analyzed by investigating their radial brightness distribution along lines centered on the knots and pointing in different directions. Each selected CK is subdivided into sectors, which include all the pixels with an angle $\alpha \pm \Delta\alpha$ from the line that connects the knot center with the position of the central star (Fig. 1). Positive (or negative) values of α correspond to pixels that are to the left (or right) of this central line. Within each sector, the Hα surface brightness $\Sigma(r)$ is determined as the average surface brightness of all pixels that lie within a distance r and $r + \Delta r$ from the center of the knot. Here we adopt $\Delta\alpha = 10°$ and $\Delta r = 1$ pixel.

3.1. *The Radial Brightness Distribution*

Figure 2 shows $\Sigma(r)$ for a typical knot, H352-815, in different directions α. Within the central dark knot region, Σ increases with increasing r and reaches a maximum Σ_{max} at a distance R_k, which we identify with the location of the ionization front and the outer edge of the neutral knot. In the following discussion, we define the luminous material outside of R_k as the cusp of a knot. Within the cusp region outside of R_k, the surface brightness decreases until the constant background brightness Σ_{bg} is reached. The solid and dashed lines in Figure 2 show the best-fitting exponential and r^{-3} brightness distribution, respectively. The scale height h of the best-fitting exponential profile $\Sigma \sim \exp[-(r - R_k)/h]$ is determined by a linear least-squares fit of $\ln(\Sigma - \Sigma_{bg})$ versus $(r - R_k)$ in the region outside of R_k. For all fits the same background brightness of $\Sigma_{bg} = 2.1 \times 10^7$ photons cm^{-2} s^{-1} sr^{-1} is adopted. Note that the exponential profile fits the data somewhat better than the r^{-3} profile, which predicts a decay of the Hα intensity that is somewhat less steep than observed.

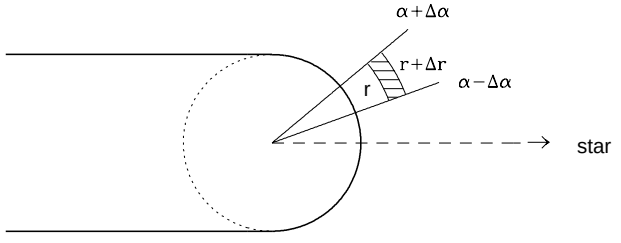


FIG. 1.—Visualization of the geometry of the measurements. The average surface brightness of all pixels that lie within a sector (α, $\alpha \pm \Delta\alpha$) and within a distance interval (r, $r + \Delta r$) (*shaded area*) determines the surface brightness $\Sigma(\alpha, r)$.

We find a very similar structure for the other knots of our sample. An exponential profile always provides an excellent fit through the data points. The r^{-3} profile, on the other hand, leads to a decrease in the intensity that is not steep enough in most cases. In order to quantify this result, we have determined the index n of the best-fitting power-law distribution $\Sigma \sim r^{-n}$ by a linear least-squares fit of $\log(\Sigma - \Sigma_{bg})$ versus $\log(r - R_k)$. Figure 3 shows n versus R_k/h for all the knots and for all directions α shown in Figure 2. A power-law profile in most cases can fit the data as well as the exponential profile. However, the best-fitting power-law index n deviates from the value $n = 3$ expected for a steady-state outflow. In most cases, n is larger than 3, in agreement with the previous conclusion that the observed profiles decrease more steeply than expected for an r^{-3} profile. Note that the maximum brightness points must be suspect, as they might be affected by the convolutions of sharp edges with the instrumental resolution. We have therefore performed test calculations that demonstrate that the results do not change even if one neglects the maximum brightness points.

The dashed line in Figure 3 shows the expected values of n versus R_k/h if the inner region ($R_k \le r \le R_k + h$) of an exponential profile $\Sigma \sim \exp[-(r - R_k)/h]$ is fitted by a power-law profile. The good agreement of the dashed line with the distribution of the data points strongly indicates that the observed profiles are indeed exponential, the scale height h being the more physical quantity. The power-law index n is an approximation, determined by the power-law fit of the inner regions of the exponential profile.

3.2. *Physical Properties of Knots*

Figure 4 shows the variation of the different physical quantities, defined in § 3.1, as a function of α for H352-815 (*solid line*) and for two additional knots, H478-801 (*dashed line*) and H386-749 (*dotted line*). Σ_{max} decreases with increasing absolute value of α, roughly as $\Sigma_{max} \sim \cos^{0.6}(\alpha)$. Because of irregularities in the shape of the cusps, the maximum value of Σ_{max} is not always reached at $\alpha = 0°$. As discussed by OH96, the apex surface brightness decreases systematically with the central star distance. The right panel of Figure 4 shows the core size R_k and the cusp scale height h as function of α for all three knots. The value of h is the same for all knots, while R_k varies by more than a factor of 2. Figure 5 demonstrates for all the knots in our sample that the cusps of all the knots have the same universal scale height, $h \approx 2$ pixels, which is also independent of direction α.

3.3. *The Importance of the Instrumental PSF for These Results*

The *HST* WFPC2 has a superb but finite point-spread function (PSF) that is dominated by the diffraction limit of the primary mirror. We have evaluated the effect of the PSF

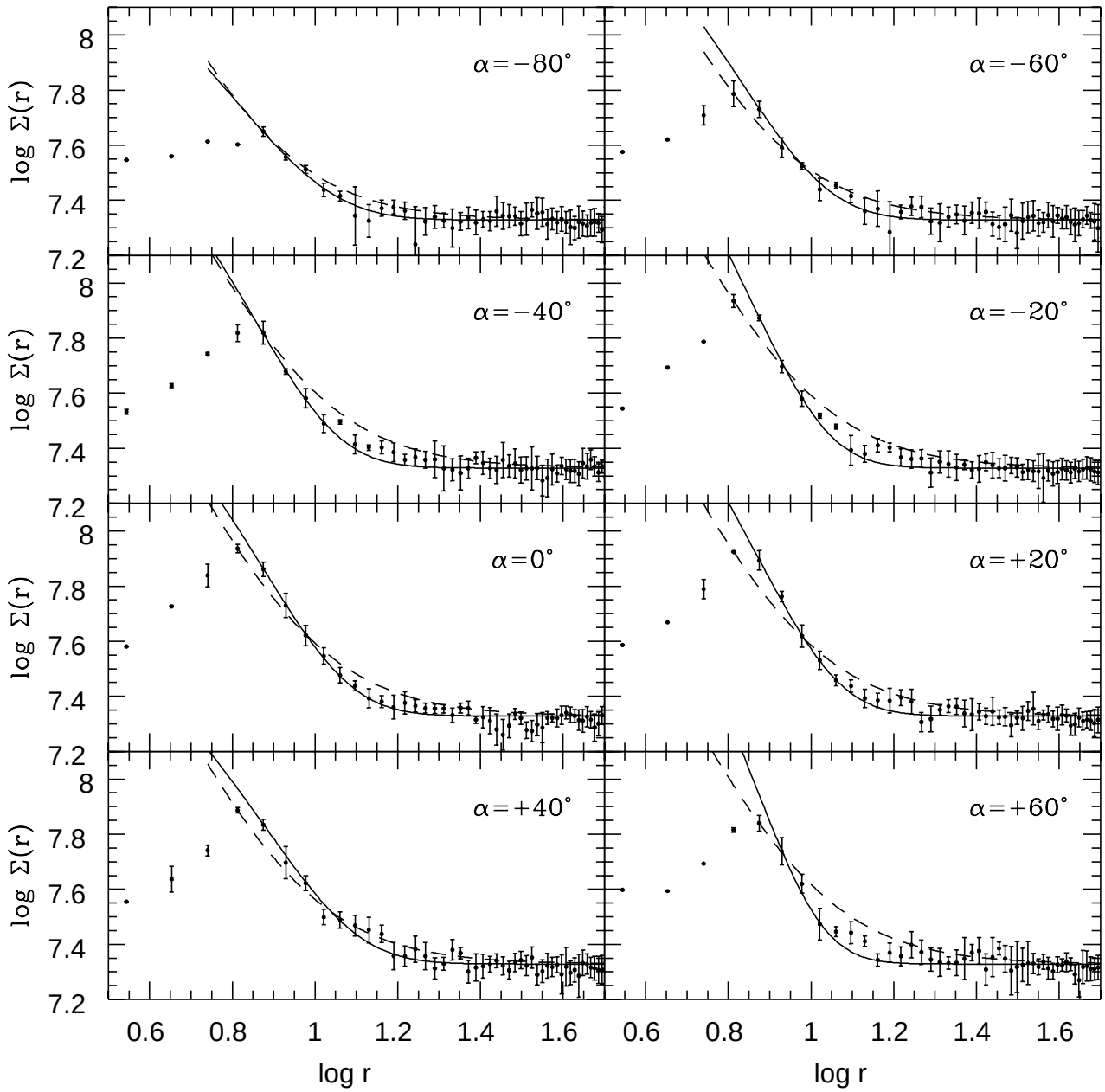


FIG. 2.—Hα surface brightness Σ as function of distance r from the center of the knot is shown for H352–815 for different directions α. The solid and dashed lines show the best-fitting exponential and r^{-3} profiles, respectively.

by constructing a model bright cusp of a CK and convolving this model image with the PSF calculated using the Tiny Tim program, provided by the Space Telescope Science Institute. The simplest model cusp is composed of a chevron of 7 constant brightness pixels, where the central three are in line and the outer ones are staggered back at a 45° angle. This would be illustrative of a CK with a cusp so concentrated that all of the light falls into one pixel. The resulting image after convolution with the PSF is shown in Figure 6 by filled circles, where we can see that the profile would drop off very rapidly, with an initial scale height of about 3/4 pixel. We also considered models that had intrinsic exponential brightness distributions with scale heights of 1, 2, 2.5, and 3 pixels. These have convolved scale heights of about 1.2, 2.5, 3.1, and 3.8; i.e., the PSF slightly increases the scale height of the brightness profile. Finally, a model with an r^{-3} distribution would give an observed profile that is fitted with a scale height of about 4.

Comparison of the results of this model with the observations indicates that certainly the CK are not characterized by an r^{-3} intrinsic brightness distribution. It also means that our characteristic derived scale heights of about 2 pixels are probably larger than the intrinsic scale heights by a few tenths.

4. DISCUSSION

The origin and future of the CK are questions that have not been resolved up to now. The Helix Nebula formed when the red giant star lost its envelope in a dense AGB wind. According to the interacting stellar winds model, the star subsequently evolved to higher temperatures, generating a fast, low-density wind (Kwok 1982; Völk & Kwok

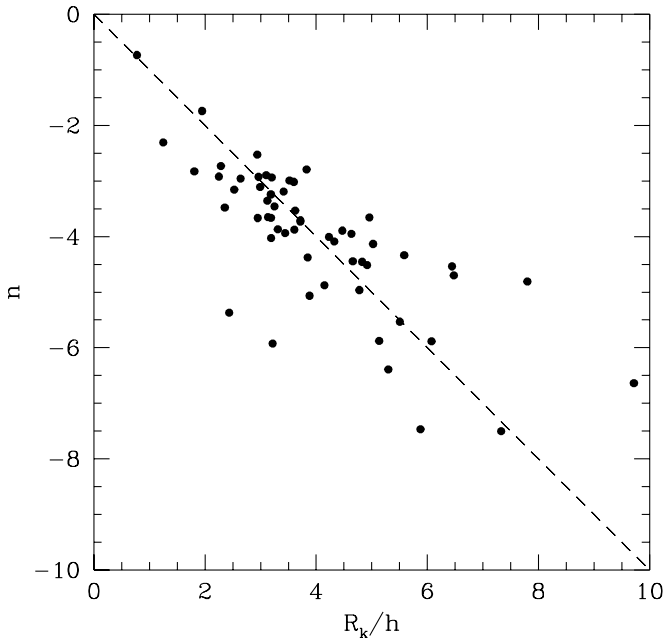


FIG. 3.—Best-fitting power-law index n for different directions α and for all the knots of the present sample, shown as a function of the normalized knot radius R_k/h in the direction α. The dashed line shows the expected values of n if the power-law profile is fitted to the inner region of the exponential profile $\Sigma \sim \exp[-(r - R_k)/h]$.

1985) that dissipated its kinetic energy at an inner shock front, creating a hot, inner bubble with temperatures of $T \approx 10^6$ K and densities of $n \approx 1$ cm^{-3}. The Helix Nebula is currently in this evolutionary stage, where the cold and dense AGB shell with expansion velocities on the order of 10 km s^{-1} is swept up by the inner hot bubble with radial velocities on the order of 20 km s^{-1}. The CK might originate from density inhomogeneities within the dense shell that are excavated and left behind when the hot gas pushes the slowly moving shell outward. This model provides an explanation for the observed expansion velocities of the CK, on the order of 10 km s^{-1}, which are smaller than the overall expansion velocity of the nebula, which is on the order of 24 km s^{-1} (Meaburn et al. 1996).

According to this scenario, the CK should be embedded in a hot, dilute gas that flows around the knots with relative velocities on the order of 10 km s^{-1}. Stripping the outermost parts of their luminous cusps would naturally lead to cometary tails pointing radially away from the center. The cusps result from photoionization of the neutral knot surfaces by the UV field of the central star.

Our analysis demonstrates clearly that the cusps have exponential surface brightness profiles. This result is puzzling, since standard outflow models of photoionized, spherical surfaces predict an inner, freely expanding ionization region with an r^{-2} density distribution, leading to an r^{-3} surface brightness profile (Henney et al. 1996; Dyson 1968). Note, however, that the ionization region expands into the high-temperature surrounding, which moves with a relative velocity on the order of 10 km s^{-1}. At some distance from the knots, the external pressure should be able to stop the expansion of the ionization front. Numerical calculations (Henney et al. 1996) show that an inner, undisturbed, freely expanding region with an r^{-2} density distribution would exist even in this situation. The size of this region is expected to be on the order of $l \approx 3 \times 10^{15}$ cm (Burkert & O'Dell 1998), and the timescale for the power-law profile to be established is on the order of $\tau = l/c_i \approx 100$ yr, where $c_i \approx 10$ km s^{-1} is the sound speed of the ionized gas. Since τ is much shorter than the age of the knots, we would expect to find an r^{-3} surface brightness profile, in contradiction to the observations.

OH96 have demonstrated that the CK are likely to be ionization bounded. All the UV photons from the central star are absorbed in the ionization region. If the cusps could also be pressure confined by an external hot surrounding medium, they might actually represent ionized atmospheres in hydrostatic equilibrium rather than freely expanding ones. Adopting a constant temperature on the order of 10^4 K within the ionization region, one would also expect a

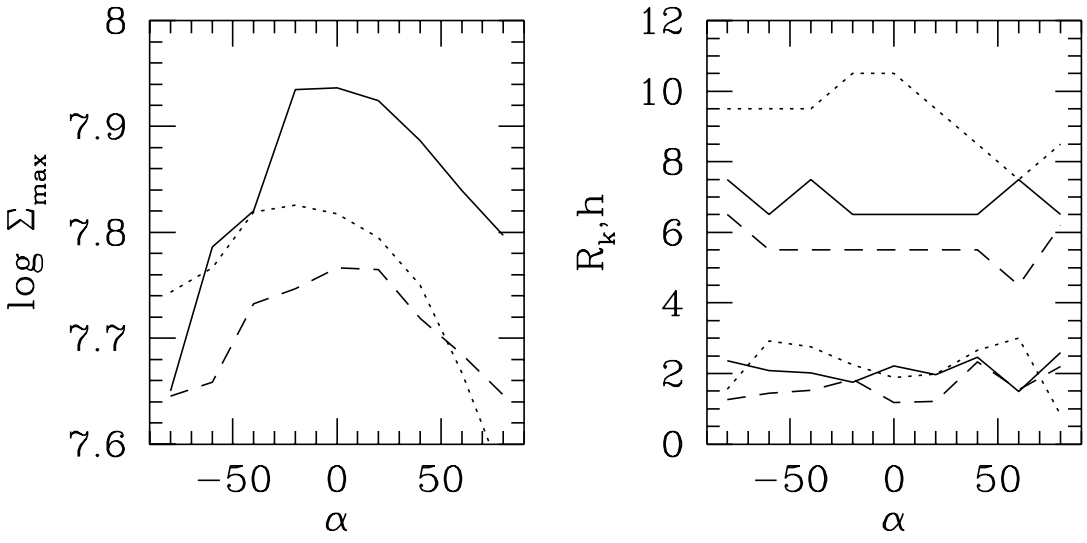


FIG. 4.—*Left panel*: Variation of the maximum cusp surface brightness Σ_{max} in units of photons cm^{-2} s^{-1} sr^{-1} as a function of direction α. *Right panel*: neutral knot radius R_k (*upper three curves*) and exponential cusp scale height h (*lower three curves*) as function of α for knots H352-815 (*solid lines*), H478-801 (*dashed lines*) and H386-749 (*dotted lines*).

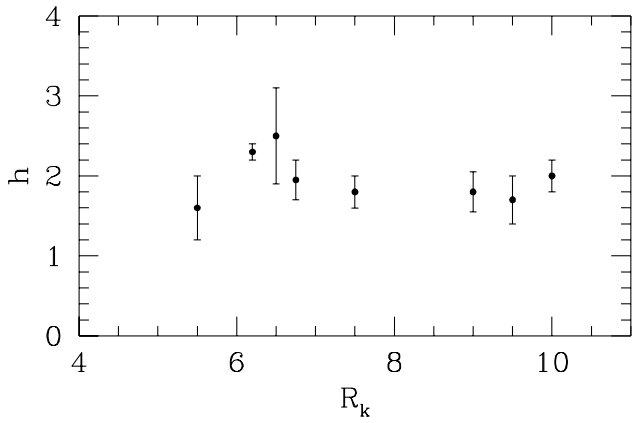


FIG. 5.—Exponential cusp brightness scale heights h are shown as a function of the knot radius R_k. The error bars indicate the total variation of h as function of α for a given knot.

constant cusp density rather than an exponential density distribution. The observations therefore indicate the existence of an additional force that must act isotropically, leading to exponential profiles with constant scale heights.

The gravitational force of the knots is negligible, given their small masses, which are only on the order of 3×10^{-5} $M_\odot$ (O'Dell & Burkert 1997). Heat conduction from the hot environment into the colder cusps could lead to a temperature gradient and by this, in pressure equilibrium, also to a density gradient. For average temperatures $T \approx 10^4$ K and densities $n \approx 1000$ cm^{-3}, the scale length λ on which the temperature and density would change as a result of conduction is $\lambda = 6.4 \times 10^{14}$ $(T/10^4$ K$)^{1.48}(n/\mathrm{cm}^3)^{-1}$ cm $\approx 6.4 \times 10^{11}$ cm (McKee & Cowie 1977), which is orders of magnitude smaller than the observed scale height.

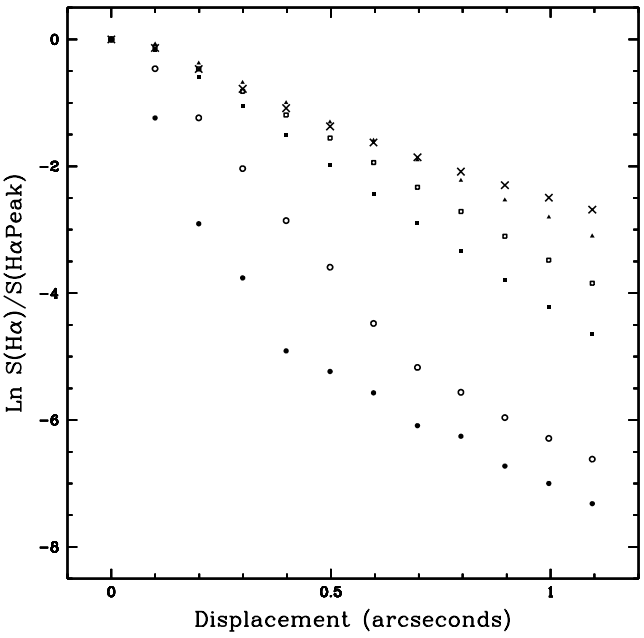


FIG. 6.—Results of convolving model bright cusps with the PSF of the system used for observing the CK. The filled circles show a cusp with all of the light in a single pixel, the open circles show a cusp with an exponential brightness distribution with a scale height of 1; filled squares, open squares, and filled triangles are similar, for scale heights of 2, 2.5, and 3 pixels, respectively. Crosses indicated the observed brightness distribution expected for an r^{-3} intrinsic brightness distribution.

4.1. Lyα *Photon Radiation Pressure as an Explanation for the Confinement*

It is possible that the structure of the atmospheres of the CK results from radiation pressure of Lyα photons acting on the cusp atmosphere material, a process explained more completely in a discussion of the proplyds found in the Orion Nebula (O'Dell 1998). The attraction of this process is that it is an available force whose magnitude can be large enough to be important and that will be isotropic, which appears to be required by our analysis of the cusp atmospheres.

If the observed exponential brightness is an indicator of an atmosphere in hydrostatic equilibrium, then the magnitude of the confining pressure must be equal to the local pressure at the base of the atmosphere. The more familiar formulation of this statement as it applies to the Earth's atmosphere is that the pressure at the bottom of the atmosphere is equal to the weight of the overlying column of material. OH96 showed that direct radiation pressure from the central star failed this test by many orders of magnitude, and we now know that the asymmetry in confinement by such a mechanism would be in contradiction to what is observed. However, the radiation pressure from trapped Lyα photons can be much greater than photons directly traveling from the star, because the Lyα photons are trapped by their short mean free path. Since the ratio of absorption coefficients in the center of the Lyα line and in the Lyman continuum is about 10^4 and the Helix Nebula as a whole is ionization bounded, the mean free path of the Lyα photon that results from each recombination is a small fraction of the size of the Nebula. These photons travel randomly about until they are absorbed by a dust grain or succeed in escaping when reemitted far from the frequency of the line center.

The radiation density of Lyα photons will be 1/3 of the energy density ($\rho_{\mathrm{Ly}\alpha}$), which is given by

$$\rho_{\mathrm{Ly}\alpha} \leq \alpha_B N_e N_p E_{\mathrm{Ly}\alpha} \frac{R}{c} q \,, \qquad (1)$$

where N_p is the proton density, which is about equal to the electron density N_e, $E_{\mathrm{Ly}\alpha}$ is the energy in a Lyα photon, q is the number of times a Lyα photon is scattered, α_B is the hydrogen recombination rate whose magnitude is 2.59×10^{-13} cm^3 s^{-1} at T_e (Osterbrock 1989), and R is the linear size of the photon-emitting region. The equation gives an upper limit, since the actual total path length traversed will be ql, not qR, where l is the mean free path for Lyα photons, which is much shorter than R.

The ratio of the confining pressure to the cusp base pressure ($N_0 kT_e$) will be $\beta \leq 1.68 \times 10^{-23}$ $R(N_p N_e q/N_0)$. Inserting the values of $R = 10^{18}$ cm, $N_p N_e = 3600$ cm^{-6}, and $N_0 = 1600$ cm^{-3} from O'Dell & Burkert (1997), one finds $\beta \leq 3.8 \times 10^{-5}$ q. In a nebula where the dust-to-gas ratio is about equal to the general interstellar medium, absorption of Lyα photons by dust can become the determining factor for q, with absorption occurring typically when q times the mean free path has become about 10^4 R. Hummer & Kunasz (1980) have calculated the case of Lyα photons resonantly scattered in a dusty medium and find that $q \simeq 10^4$ for a continuum optical depth of unity, which

means that β will have a value of much less than unity.

The mechanism that we consider for confining the CK atmospheres is the action of the absorption and transfer of momentum of the Lyα photons as one proceeds toward the surface of the CK. If the dust-to-gas ratio remains constant throughout the outer CK, there will be a constant ratio of force per unit mass, a necessary condition for hydrostatic equilibrium with a constant scale height. The scale height for the atmospheric density would be $H = 6kT_e/\sigma\rho_{\mathrm{Ly}\alpha}$, where σ is the dust extinction cross section per hydrogen atom, about 5×10^{-22} cm^2 (Osterbrock 1989). Inserting the previous numerical values then gives $H \geq 3.7 \times 10^{22}$ cm. The surface brightness scale height of 2 pixels requires a density scale height of 1.27×10^{15} cm, which would require $q \geq 3 \times 10^7$, which vastly exceeds the value predicted by Hummer & Kunasz's (1980) predictions. This means that this mechanism also fails to explain the scale height observed. It is unlikely that the flow of nebular gas passing the CK (Meaburn et al. 1998) is the source of confinement, since its kinetic pressure is about 2 orders of magnitude less than the Lyα pressure.

Unfortunately, this leaves us in the situation of being able to see that the atmospheres are quite compressed and that the CK have lost so little mass that they still exist, but having no mechanism to explain their confinement. Without knowledge of the process causing the confinement, the challenging theoretical problem of predicting the further evolution of these objects as the central star cools remains entirely uncertain.

Shui-Kwan Wong ably assisted in the derivation of the calibration constants. This work was supported in part by NASA grant NAG5-1626 to Rice University and by the German Humboldt Foundation while the second author was a guest of the Max Planck Institute for Astronomy in Heidelberg.

REFERENCES

Burkert, A., & O'Dell, C. R. 1998, in preparation
Dyson, J. E. 1968, Ap&SS, 1, 388
Handron, K. D. 1995, M.S. thesis, Rice Univ.
Harris, H. 1997, in IAU Symp. 180, Planetary Nebulae, ed. H. Habing (Dordrecht: Reidel), in press
Henney, W. J., Raga, A. C., Lizano, S., & Curiel, S. 1996, ApJ, 465, 216
Huggins, P. J., Bachiller, R., Cox, P., & Forveille, T. 1992, ApJ, 401, L43
Hummer, D. G., & Kunasz, P. B. 1980, ApJ, 236, 609
Kwok, S. 1982, ApJ, 258, 280
Meaburn, J., Clayton, C. A., Bryce, M., & Walsh, J. R. 1996, MNRAS, 281, L57
Meaburn, J., Clayton, C. A., Bryce, M., Walsh, J. R., Holloway, A. J., & Steffen, W. 1998, MNRAS, in press
Meaburn, J., Walsh, J. R., Clegg, R. E. S., Walton, N. A., Taylor, D., & Berry, D. S. 1992, MNRAS, 255, 177
McKee, C. F., & Cowie, L. L. 1977, ApJ, 215, 213
O'Dell, C. R. 1998, AJ, submitted
O'Dell, C. R., & Burkert, A. 1997, in IAU Symp. 180, Planetary Nebulae, ed. H. Habing (Dordrecht: Reidel), in press
O'Dell, C. R., & Handron, K. D. 1996, AJ, 111, 1630 (OH96)
Osterbrock, D. E. 1989, Astrophysics of Gaseous Nebulae and Active Galactic Nuclei (Mill Valley: Univ. Science Books)
Völk, K., & Kwok, S. 1985, A&A, 153, 79
Vorontzov-Velyaminov, B. A. 1968, in IAU Symp. 34, Planetary Nebulae, ed. D. E. Osterbrock & C. R. O'Dell (Dordrecht: Reidel), 256
Walsh, J. R., & Meaburn, J. 1993, Messenger, 73, 35
Young, K., Cox, P., Huggins, P. J., Forveille, T., & Bachiller, R. 1997, ApJ, 482, L101